Activation of phosphatidylinositol 3-kinase signaling by a mutant thyroid hormone β receptor

Fumihiko Furuya*, John A. Hanover†, and Sheue-yann Cheng*‡

*Laboratory of Molecular Biology, Center for Cancer Research, National Cancer Institute, and †Laboratory of Cellular Biochemistry and Biology, National Institute of Diabetes and Digestive and Kidney Diseases, National Institutes of Health, Bethesda, MD 20892

Communicated by Ira H. Pastan, National Institutes of Health, Bethesda, MD, December 15, 2005 (received for review October 4, 2005)

Activation of the phosphatidylinositol 3-kinase (PI3K)–AKT/protein kinase B signaling pathway has been associated with multiple human cancers. Recently we showed that AKT is activated in both the thyroid and metastatic lesions of a mouse model of follicular thyroid carcinoma [thyroid hormone β receptor (TRβ)$^{PV/PV}$ mice]. This TR$\beta^{PV/PV}$ mouse harbors a knock-in mutant TRβ gene (TRβPV mutant) that spontaneously develops thyroid cancer and distant metastasis similar to human follicular thyroid cancer. Here we show that in thyroid tumors, PV mutant bound significantly more to the PI3K-regulatory subunit p85α, resulting in a greater increase in the kinase activity than did TRβ1 in wild-type mice. By GST pull-down assays, the ligand-binding domain of TR was identified as the interaction site with p85α. By confocal fluorescence microscopy, p85α was shown to colocalize with TRβ1 or PV mainly in the nuclear compartment of cultured tumor cells from TR$\beta^{PV/PV}$ mice, but cytoplasmic p85α/PV or p85α/TRβ1 complexes were also detectable. Further biochemical analysis revealed that the activation of the PI3K–AKT–mammalian target of the rapamycin–p70^{S6K} pathway was observed in both the cytoplasmic and nuclear compartments, whereas the activation of the PI3K–integrin-linked kinase–matrix metalloproteinase 2 pathway was detected mainly in the extranuclear compartments. These results suggest that PV, via the activation of p85α, could act to affect PI3K downstream signaling in both the nuclear and extranuclear compartments, thereby contributing to thyroid carcinogenesis. Importantly, the present study unveils a mechanism by which a mutant TR acts to activate PI3K activity via protein–protein interactions.

mouse model | mutant thyroid hormone receptor | thyroid carcinogenesis

Thyroid cancer, the most common form of endocrine malignancy, has many different subtypes, with the most common being papillary and follicular carcinomas. Follicular thyroid carcinoma is typically a well differentiated cancer, but it has a greater tendency than papillary cancer to metastasize to distant sites. Distance metastasis predicts a poor response to treatment and subsequent progression and mortality from thyroid cancer. The molecular mechanisms underlying the initiation and progression of thyroid cancer are not fully understood, but it is generally believed that dysregulation of cell growth and cell death are involved.

Evidence has shown that dysregulation of phosphatidylinositol 3-kinase (PI3K) signaling contributes to abnormal cell growth and cellular transformation in a variety of neoplasms, including thyroid cancer. PI3K is a kinase consisting of a M_r 85,000 regulatory subunit and a M_r 110,000 catalytic subunit. Upon activation by membrane receptors, PI3K phosphorylates phosphatidylinositol-4,5-bisphosphate to form phosphatidylinositol-3,4,5-triphosphate [PtdIns(3,4,5)P_3]. Through phosphoinositol-dependent kinases, the downstream effectors of PI3K, AKT/protein kinase B (a serine and threonine kinase) is phosphorylated and activated to further phosphorylate other downstream protein substrates, thus leading to various signaling cascades that affect cellular functions (1–3). The activity of PI3K is negatively regulated by PTEN, a protein phosphatase that removes a phosphate group from PtdIns(3,4,5)P_3 (4).

Recent studies have indicated that aberrant PI3K–AKT signaling is associated with thyroid carcinogenesis. Patients with the autosomal dominant Cowden's syndrome have mutations in PTEN, leading to overactivation of AKT, and they develop both benign and malignant follicular tumors, including follicular thyroid carcinoma, along with other cancers (5–7). Studies of human thyroid cancer specimens by several groups have shown AKT overexpression and overactivation in primary thyroid cancers (8, 9). This enhancement of AKT activity is more predominant in follicular thyroid cancers and in thyroid cancer cells invading tumor capsules than in those localized to central, less invasive regions (10).

Recently, using a mouse model of follicular thyroid carcinoma [thyroid hormone β receptor (TRβ)$^{PV/PV}$ mouse], we found that AKT is also overactivated in thyroid tumors (11–14). Similar to that observed in human thyroid cancer, AKT was overexpressed and phosphorylated AKT was detected in primary tumors and the metastases (11). The TR$\beta^{PV/PV}$ mutant mouse was created by a targeted mutation of TRβ (TRβPV) by means of homologous recombination and the Cre-LoxP system (15). The TRβ mutant (denoted as PV) was identified in a patient (PV) with resistance to thyroid hormone (16). Resistance to thyroid hormone is caused by mutations of the TRβ gene and manifests symptoms as a result of decreased sensitivity to the thyroid hormone (T3) in target tissues (17). PV has a C-insertion at codon 448 that produces a frame shift in the C-terminal 14 aa of TRβ1 (16). PV has completely lost T3 binding and exhibits potent dominant-negative activity (18). Remarkably, as TR$\beta^{PV/PV}$ mice age, they spontaneously develop follicular thyroid carcinoma similar to human thyroid cancer, with pathological progression from hyperplasia to vascular invasion, capsular invasion, anaplasia, and eventually metastasis (12–14). However, the molecular pathways leading to the activation of AKT have not been elucidated.

In the present study, we sought to understand the molecular mechanisms underlying the activation of AKT signaling during thyroid carcinogenesis in TR$\beta^{PV/PV}$ mice. We found that p85α recruited TRβ1 or mutant PV, but with a significantly higher affinity for the latter. The association of PV with p85α results in a marked activation of PI3K activity. Furthermore, p85α was colocalized with TRβ1 or mutant PV not only in the cytoplasm, but also in the nucleus of thyroid tumor cells. The sequestering of PV by p85α in both the nuclear and extranuclear compartments allowed PV to activate various PI3K downstream signaling cascades, affecting divergent cellular functions.

Results

Activation of PI3K Signaling in the Thyroid of TR$\beta^{PV/PV}$ Mice. To elucidate the underlying molecular mechanisms by which the mutant PV activates AKT activity, we first examined the activity in the thyroid of its upstream kinase, PI3K, comparing wild-type and

Conflict of interest statement: No conflicts declared.

Abbreviations: ILK, integrin-linked kinase; MMP, matrix metalloproteinase; mTOR, mammalian target of rapamycin; PARP, poly ADP-ribose polymerase; PDI, protein disulfide isomerase; PI3K, phosphatidylinositol 3-kinase; TRβ, thyroid hormone β receptor; PV, TRβ mutant; PtdIns(3,4,5)P_3, phosphatidylinositol-3,4,5-triphosphate.

‡To whom correspondence should be addressed at: Laboratory of Molecular Biology, National Cancer Institute, 37 Convent Drive, Room 5128, Bethesda, MD 20892-4264. E-mail: chengs@mail.nih.gov.

www.pnas.org/cgi/doi/10.1073/pnas.0510849103

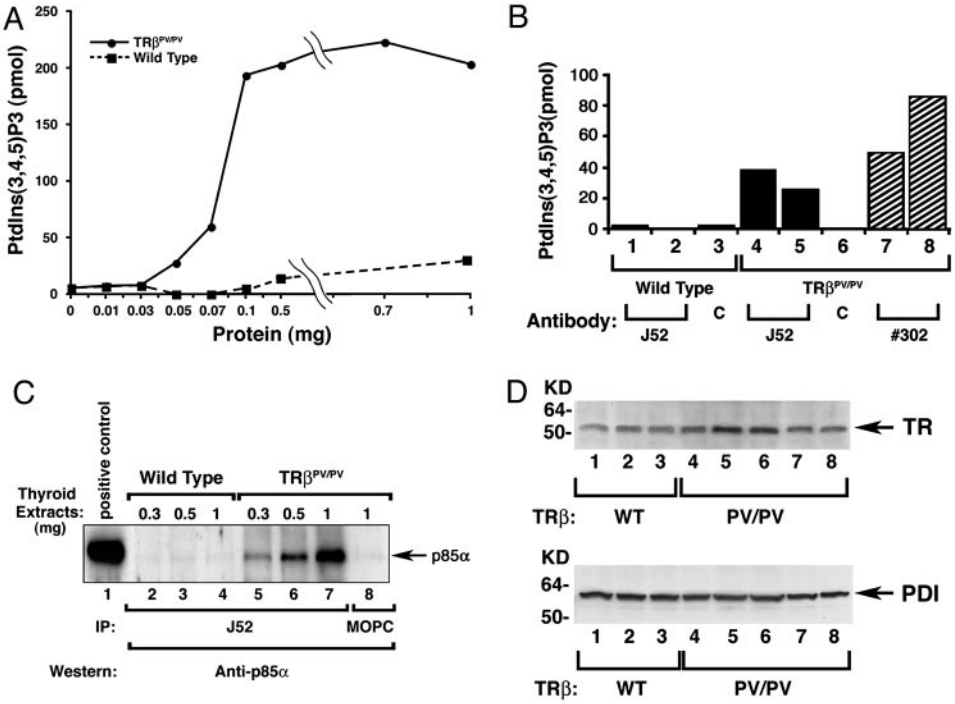

Fig. 1. Activation of PI3K activity in the thyroid extracts of TR$\beta^{PV/PV}$ mice. (*A*) Increasing concentrations as marked of total thyroid extracts from wild-type mice (solid squares) and TR$\beta^{PV/PV}$ mice (solid circles) were immunoprecipitated with anti-p85α antibody. PI3K activity of precipitates from each concentration was measured by ELISA, as described in *Materials and Methods*, and expressed as the relative production of PtdIns(3,4,5)P_3 by each sample. (*B*) One hundred micrograms of proteins derived from the total thyroid extracts of wild-type mice (bars 1–3; three mice) or TR$\beta^{PV/PV}$ mice (bars 4–8) were immunoprecipitated with 5 μg of anti-TRβ1 (J52, bars 1 and 2, wild-type mice; bars 4 and 5, two TR$\beta^{PV/PV}$ mice), anti-PV (#302, bars 7 and 8, two mice) antibodies, or an irrelevant monoclonal antibody (MOPC) as control (bars 3 and 6, marked as C). PI3K activities in the immunoprecipitates were measured by ELISA, as described in *Materials and Methods*. (*C*) Three hundred, 500, or 1,000 μg of pooled protein lysates from thyroid extracts of six wild-type mice or three TR$\beta^{PV/PV}$ mice, respectively, was immunoprecipitated with J52 antibody and subjected to immunoblot analysis probed with anti-p85α antibody (catalog no. 06-195). Lane 1 shows Jurkat cell lysate (catalog no. 12-303; Upstate Biotechnology) as a positive control. (*D Upper*) The abundance of TRβ1 and PV receptor proteins in the thyroids of wild-type mice (lanes 1–3) and TR$\beta^{PV/PV}$ mice (lanes 4–8), respectively. The loading control (*D Lower*) used PDI.

TR$\beta^{PV/PV}$ mice. PI3K was immunoprecipitated from thyroid extracts by using antibody against the regulatory subunit p85α followed by kinase assays. Fig. 1*A* shows the concentration-dependent increased kinase activity from thyroid extracts of TR$\beta^{PV/PV}$ mice. In contrast, the immunoprecipitates from extracts of wild-type mice exhibited very low activity. Recent studies indicate that PI3K is associated with TRβ in human vascular endothelial cells and fibroblasts (19, 20). We therefore used monoclonal antibody J52 (21), which recognizes the N-terminal region of the A/B domain of TRβ1 and PV, to determine whether these two TRs are associated with PI3K. Fig. 1*B* shows that antibody J52 precipitates from thyroid extracts of two TR$\beta^{PV/PV}$ mice (Fig. 1*B*, bars 4 and 5) had $\approx$30-fold more PI3K activity than did wild-type mice (bars 1 and 2). The increased PV-associated PI3K activity was not due to preferential binding of J52 with PV, because J52 interacted with TRβ1 and PV with a similar affinity (data not shown). To be certain that the increased PI3K activity was due to its association with PV, the same tumor extracts were first precipitated with monoclonal antibody that specifically recognizes the C-terminal PV sequence (#302) (22) followed by kinase determination. As shown in bars 7 and 8 (two mice, Fig. 1*B*), a 26- to 85-fold increase in kinase activity was detected. The fact that no PI3K activity was observed in the controls by immunoprecipitation of thyroid extracts with an irrelevant mouse antibody MOPC (bars 3 and 6) demonstrated the specificity shown in bars 1, 2, 4, 5, 7, and 8. The differences in fold of increases in PI3K activity between the J52 immunoprecipitates (the epitope is located in the A/B domain of PV) and #302 immunoprecipitates (the epitope is located in the C-terminal 16 aa of PV) reflected the differences in the binding affinity of these two antibodies with PV.

The marked increase in PI3K activity associated with PV prompted us to determine whether more PI3K protein was bound to PV than to TRβ1. We used antibody J52, which recognizes the same epitope of PV and TRβ1 with similar affinity, to immunoprecipitate the receptors in the thyroid tumor extracts followed by Western blotting with anti-p85α antibodies. The PI3K p85α regulatory subunit was detected in a concentration-dependent manner in TR$\beta^{PV/PV}$ mice (Fig. 1*C*, lanes 5–7), but not in wild-type mice (Fig. 1*C*, lanes 2–4) and not when an irrelevant antibody MOPC was used (lane 8). These results indicate that more PV in the thyroid of TR$\beta^{PV/PV}$ mice was bound to p85α than TRβ1 in wild-type mice. Because PI3K activity is negatively regulated by PTEN (4), we also determined the abundance of PTEN proteins in the thyroid extracts. No significant differences in PTEN protein abundance were detected in the thyroids of wild-type and TR$\beta^{PV/PV}$ mice, indicating that the increased PI3K activity is not due to the repression by PTEN (data not shown). Using thyrocytes prepared from wild-type and TR$\beta^{PV/PV}$ mice, we found that neither thyroid-stimulating hormone nor T3 had effects on the p85α protein level and its interaction with PV (data not shown).

The increase in the binding of PV to PI3K that is shown in Fig. 1*C* was not due to increased PV protein abundance in the thyroid of TR$\beta^{PV/PV}$ mice. As shown by Western blot using antibody J52 (Fig. 1*D Upper*), the abundance of TRβ1 protein in the thyroid of wild-type mice (lanes 1–3 for three mice) and of PV protein in the thyroid of TR$\beta^{PV/PV}$ mice (lanes 4–8 for five mice) was similar. The loading control using protein disulfide isomerase (PDI) is shown in Fig. 1*D Lower*. Taken together, these data indicate that PI3K had a higher avidity in recruiting PV.

GST binding assays were used to further confirm the interaction

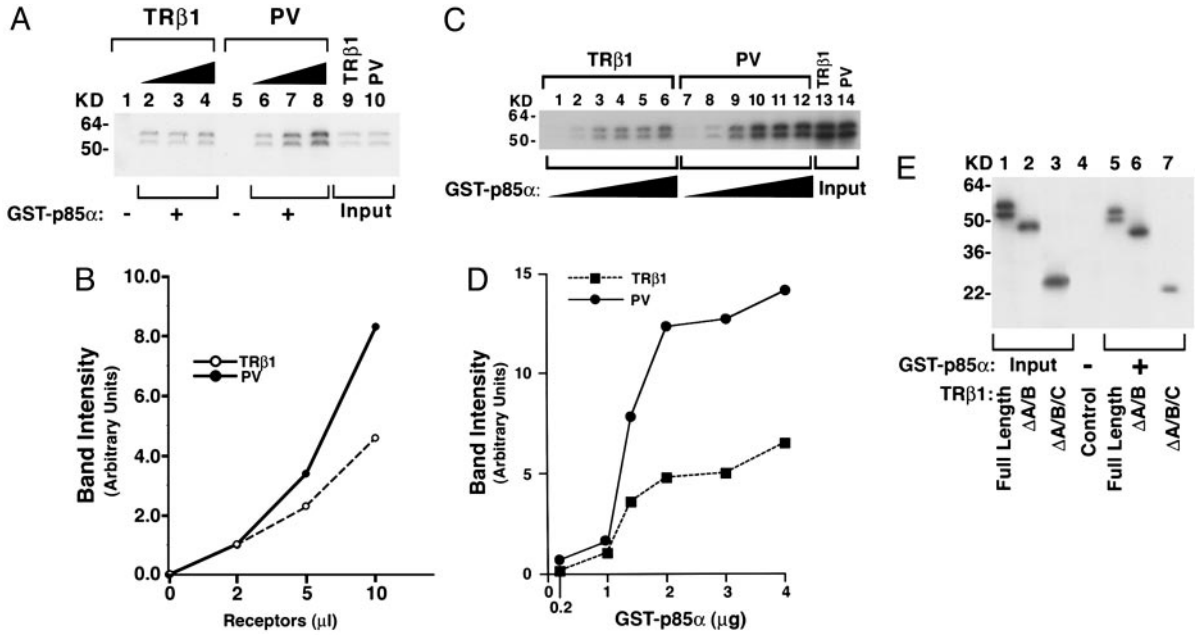

Fig. 2. p85α protein binds to PV more avidly than to TRβ1. (*A*) GST–p85α fusion protein was incubated with 2, 5, or 10 μl of ^{35}S-labeled TRβ1 (lanes 2, 3, and 4, respectively) or PV (lanes 6, 7, and 8, respectively) prepared by *in vitro* translation/transcription. Lanes 1 and 5 were from the incubation of GST with 2 μl of TRβ1 and PV, respectively. Lanes 9 and 10 show the input of *in vitro* translation/transcription samples (0.2 μl). (*B*) The band intensity was scanned and quantified by using NIH IMAGE software. (*C*) Ten microliters of ^{35}S-labeled TRβ1 (lanes 1–6) or PV (lanes 7–12) prepared by *in vitro* translation/transcription was incubated with increasing concentrations of bead-bound GST–p85α as described in *Materials and Methods*. (*D*) The band intensity was scanned and quantified by using NIH IMAGE. (*E*) Identification of the ligand-binding domain of TRβ1 as the interaction site with p85α. Five microliters of ^{35}S-labeled full-length and TRβ1 proteins lacking the A/B domain (ΔA/B) or the A/B/C domains (ΔA/B/C) was synthesized (25) by *in vitro* transcription/translation and incubated with GST–p85α, as described in *Materials and Methods*. Lanes 1–3 were the input (0.5 μl of lysates). Lanes are as marked.

of p85α with TRβ1 or PV. As shown in Fig. 2*A*, p85α bound to increasing concentrations of TRβ1 (lanes 2–4) or PV (lanes 6–8) in a concentration-dependent manner. Consistent with the findings using thyroid tissues (see Fig. 1), quantification of the intensities of the bands showed that PV bound more strongly to p85α than TRβ1 did (Fig. 2*B*). At a constant concentration of TRβ1 or PV, but with increasing concentrations of p85α, p85α bound more strongly to PV than TRβ1 did (Fig. 2 *C* and *D*). We further mapped the domains of TRβ1 that interact with p85α. As shown in Fig. 2*E*, full-length TRβ1 (lane 5), TRβ1 lacking the A/B domain (ΔA/B, lane 6), or TRβ1 lacking the A/B and the C (the DNA binding) domains (ΔA/B/C; lane 7) all bound to GST–p85α, whereas there was no binding of full-length TRβ1 to GST alone (lane 4). Lanes 1–3 show the input of full-length TRβ1, ΔA/B, and ΔA/B/C, respectively, as controls.

Subcellular Colocalization of PI3K with TRβ1 or PV. To identify the subcellular sites on which the interaction of TRs with PI3K occurred, we separated tumor extracts into nuclear and cytosolic fractions. That one fraction was not contaminated by the other was shown by the presence of respective markers. Fig. 3*A* shows that poly ADP-ribose polymerase (PARP), the nuclear marker, was present in the nuclear fraction (Fig. 3*A*, lanes 3 and 4) but not in the cytosolic fraction (lanes 1 and 2). α-Tubulin, a cytosolic marker, was detected only in the cytosolic fraction (Fig. 3*B*, lanes 1 and 2) but not in the nuclear fraction (Fig. 3*B*, lanes 3 and 4). Using these fractions, we immunoprecipitated PV with J52 followed by Western blot analysis using anti-p85α. Indeed, as shown in Fig. 3*C*, in the wild-type mice similarly low levels of p85α were detected in the thyroid nuclear fraction as well as in the nuclear fractions (lanes 1 and 3). In the thyroid of TR$\beta^{PV/PV}$ mice, a significantly higher p85α was found in the nuclear than in the cytosolic fraction (Fig. 3*C*, lanes 3 and 4). Lanes 5 and 6 and lanes 7 and 8 show the input for cytosolic and nuclear fractions, respectively. These results suggest that PI3K interacts with TRβ1 or PV in the nucleus as well as in the cytoplasm.

The subcellular colocalization of PI3K with TRβ1 or PV was visualized by confocal fluorescence microscopy by using cultured

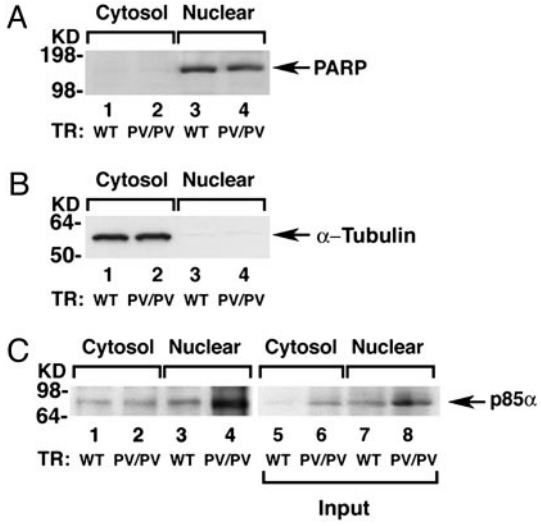

Fig. 3. p85α interacts more avidly with PV than with TRβ1 in the nuclear compartment. (*A* and *B*) The thyroid extracts of 12 wild-type mice or 3 TR$\beta^{PV/PV}$ mice were pooled and separated into nuclear or cytosolic fractions. The purity of each fraction was monitored by the respective markers, PARP for the nuclear fraction (*A*) and α-tubulin for the cytosolic fraction (*B*). (*C*) An equal amount of the nuclear or cytosolic fraction (100 μg of proteins) was immunoprecipitated with 5 μg of J52 followed by Western blot analysis using anti-p85α antibody. Lanes are as marked. Lanes 5–8 show the corresponding input of the p85α protein.

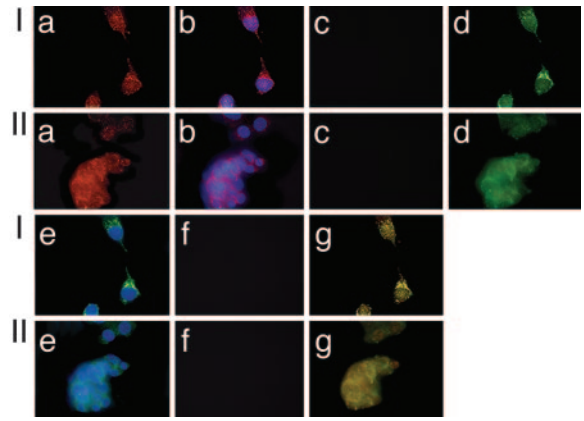

Fig. 4. p85α is colocalized with TRβ1 or PV in both the nuclear and extranuclear compartments. The primary cultured cells derived from the thyroids of wild-type mice (*I*) or TR$\beta^{PV/PV}$ mice (*II*) were fixed and incubated with anti-TRβ1 (J52) and anti-p85 antibody (SC423) followed by secondary antibody conjugated with Alexa Fluor 488 (green) or rhodamine (red), respectively, as described in *Materials and Methods*.

cells derived from the thyroid of wild-type mice and tumors of TR$\beta^{PV/PV}$ mice. As shown in Fig. 4*Ia*, the PI3K subunit p85α was detected in the nucleus as well in the cytoplasm of the wild-type mice. Fig. 4*Ib* shows the nuclei stained by DAPI. Fig. 4*Ic* shows the negative control when no primary antibody was used. TRβ1 was detected mainly in the nucleus, but there was also minor distribution in the cytoplasm (Fig. 4*Id*). Fig. 4*Ie* shows the nuclei stained by DAPI. Fig. 4*If* shows the negative control when no primary antibody was used. The colocalization of p85α and TRβ1 was shown in yellow when the two images from Fig. 4 *Ia* and *Id* were merged (Fig. 4*Ig*), indicating the colocalization of p85α and TRβ1 in both the nucleus and cytoplasm. Similar to thyroid cells from wild-type mice, p85α was localized in both the nucleus and cytoplasm of TR$\beta^{PV/PV}$ mice (Fig. 4*IIa*). PV was found to distribute mainly in the nucleus, but with significant localization in the cytoplasm. PV was shown to colocalize with p85α in both nuclear and cytoplasm compartments [merged yellow image in (Fig. 4*IIg*)]. However, we were unable to detect the localization of either TRβ1 or PV on the plasma membrane. Taken together, these results indicate that p85α interacts with TRβ1 in thyrocytes of wild-type mice and with PV in the thyroid tumor cells of TR$\beta^{PV/PV}$ mice.

Activation of PI3K Signaling by PV Occurs in both the Cytoplasm and the Nucleus. PI3K signaling is critical in mediating a variety of important cellular functions such as proliferation, apoptosis, and metastasis (23). To understand the functional consequences of interaction of PV with PI3K, we focused on two PI3K downstream signaling pathways: the AKT–mammalian target of rapamycin (mTOR)–p70^{S6K} pathway and the integrin-linked kinase (ILK) pathway. The former is known to mediate cell growth and proliferation (24), and the latter is involved in cell migration, invasion, and an inhibition of apoptosis (25–27). To identify major subcellular compartments of PV-induced PI3K activation, the thyroid extracts were separated into cytosolic and nuclear fractions followed by Western blot analyses. Fig. 5*Ba* shows the detection of a nuclear marker, PARP, in the nuclear fraction only, but not in the cytosolic fraction; Fig. 5*Bb* shows the detection of tubulin in the cytosolic fraction only, but not in the nuclear fraction. The abundance of these two markers also served as loading controls. Fig. 5*Aa* shows that, compared with wild-type mice (lanes 1 and 5), p85α protein abundance was significantly increased in both cytosolic (lanes 2–4) and nuclear (lanes 6–8) fractions. This increased abundance of p85α protein could further facilitate the binding with PV. Total AKT was slightly increased (≈1.2-fold) in the cytosolic fraction of

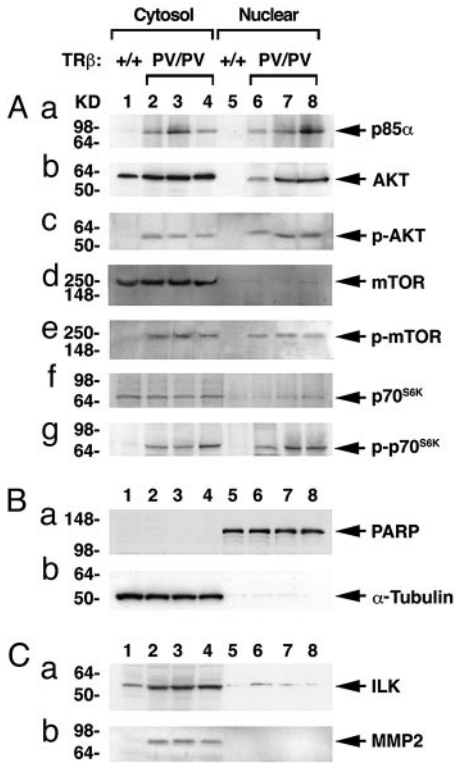

Fig. 5. Activation of the PI3K–AKT–p70^{S6K} and ILK–MMP2 pathways in the thyroid of TR$\beta^{PV/PV}$ mice. Pooled extracts from thyroids of 12 wild-type mice or 3 TR$\beta^{PV/PV}$ mice were separated into nuclear and cytosolic fractions, as described in *Materials and Methods*. Western blot analysis was carried out as described in *Materials and Methods* to determine cytosolic and nuclear abundance of the following proteins: p85α (*Aa*), AKT (*Ab*), p-AKT(S473) (*Ac*), mTOR (*Ad*), p-mTOR (*Ae*), p70^{S6K} (*Af*), and p-p70^{S6K} (*Ag*). (*B*) The expression of PARP (*a*) or α-tubulin (*b*) was used for monitoring the quality of nuclear and cytosolic fractions as well as for loading controls for the Western blot analysis shown in *A* and *C*. (*C*) Increased protein abundance of ILK (*a*) and MMP2 (*b*) in the cytosolic fraction of thyroid tumors of TR$\beta^{PV/PV}$ mice.

TR$\beta^{PV/PV}$ mice. However, whereas the total AKT was not detectable in the nuclear fraction of wild-type mice (Fig. 5A*b*, lane 5), nuclear total AKT was clearly increased in TR$\beta^{PV/PV}$ mice (Fig. 5*Ab*, compare lanes 6–8 with lane 5). Importantly, the abundance of phosphorylated AKT was significantly increased in both cytosolic and nuclear fractions of TR$\beta^{PV/PV}$ mice (Fig. 5*Ac*, lanes 2–4 and 6–8, respectively) as compared with wild-type mice (Fig. 5*Ac*, lanes 1 and 5). No apparent increase of cytosolic and nuclear mTOR (Fig. 5*Ad*, lanes 2–4 and 6–8, respectively) and p70^{S6K} (Fig. 5*Af*, lanes 2–4 and 6–8, respectively) was detected in TR$\beta^{PV/PV}$ mice as compared with wild-type mice. However, the abundance of phosphorylated mTOR (Fig. 5*Ae*, lanes 2–4 and 6–8, respectively) and p70^{S6K} (Fig. 5*Ag*, lanes 2–4 and 6–8, respectively) was significantly increased. These findings suggest that activation of PI3K by PV occurred in both the cytoplasmic and nuclear compartments.

However, as shown in Fig. 5*Ca*, lanes 2–4, the activation of ILK (one of the direct targets of PI3K activation) was detected mainly in the cytosolic fraction of TR$\beta^{PV/PV}$ mice and only very weakly in the nuclear fraction (Fig. 5*Cb*, compare lane 1 with lanes 2–4). The increased abundance of matrix metalloproteinase (MMP) 2, the direct downstream target of ILK, was detected only in the cytoplasmic fraction and not in the nuclear fraction. MMP2 is critically involved in degradation of the extracellular matrix (28, 29). Taken together, these findings suggest that PV-mediated activation of PI3K could occur in both the cytoplasmic and nuclear compartments, depending on the downstream targets.

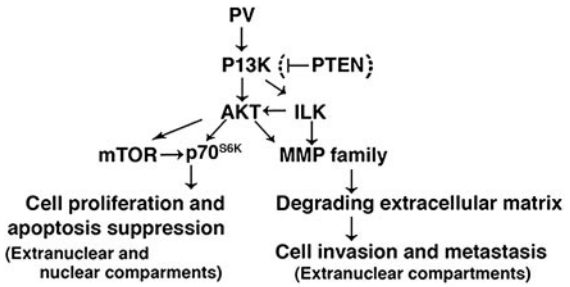

Fig. 6. Activation of PI3K signaling by PV. The physical interaction of PV with p85α results in the activation of two PI3K downstream pathways: the AKT–ILK–MMP pathway and the AKT–mTOR–p70^{S6K} pathway. The activation of the former leads to the degradation of the extracellular matrix involved in cell invasion and metastasis, and the activation of the latter results in increased cell proliferation and suppression of apoptosis. The bracket indicates that PV did not have an effect on the expression of PTEN, suggesting that PV-induced activation of PI3K is not mediated by the repression of PTEN.

Discussion

The fact that AKT is activated in a mouse model of thyroid carcinogenesis similar to human thyroid cancer provides us with a tool to understand the signaling pathways underlying the activation of AKT. Indeed, we found that both TRβ1 and PV physically interacted with p85α. However, PV bound to p85α in TR$\beta^{PV/PV}$ mice with a significantly higher affinity than TRβ1 in wild-type mice, resulting in a marked activation of PI3K activity. The increased PI3K activity led to the activation of AKT–mTOR–p70^{S6k} in both nuclear and extranuclear compartments and the ILK–MMP pathway in the extracellular compartment (see Fig. 6). The former pathway is known to increase cell proliferation and suppress apoptosis (24), and the latter is involved in the degradation of the extracellular matrix, which affects cancer cell invasion and metastasis (26, 28, 29). Given the critical role of PI3K, its activation by PV in both the nuclear and extranuclear compartments would be expected to affect the diverse downstream signaling cascades to mediate thyroid carcinogenesis. This notion is consistent with our earlier study in which cDNA microarray analysis showed complex alterations of multiple signaling pathways to be associated with thyroid carcinogenesis of TR$\beta^{PV/PV}$ mice (14).

The present study identified a TRβ mutant as an effector to modulate PI3K activity by means of protein–protein interaction. Activation of PI3K activity by means of protein–protein interaction is not without precedents. The interaction of p85α with other cellular proteins, including insulin receptor, insulin receptor substrate, and several members of the Rho family, is known to activate PI3K activity (2, 30, 31). Cao *et al.* (20) recently reported that the interaction of overexpressed TRβ1 with p85α in human fibroblasts led to the activation of the AKT–mTOR–p70^{S6K} pathway. In the thyroid of wild-type mice in which TRβ1 is the major TR isoform (14), we found that TRβ1 also interacted with p85α (Figs. 2–4). However, PI3K activity was significantly lower in wild-type mice than in TR$\beta^{PV/PV}$ mice (Figs. 1 and 5). We had mapped the interaction region of TRβ1 with p85α to be the ligand-binding domain. Because PV has a frame-shift mutation at the C terminus of TRβ1, it is reasonable to postulate that the conformational changes in this region could favor PV to interact with p85α more strongly than TRβ1. The interaction of another TRβ mutant, G345R, with p85α has been reported in human fibroblasts (20). In this study, the overexpressed TRβ1 and TRβG345R by means of adenoviral infection bound equally well with p85α. However, in contrast to PV, TRβG345R is unable to activate PI3K activity (20). These findings suggest that the conformation of TRβ1 at the carboxyl end of the ligand-binding domain is critical for the interaction with p85α and the activation of PI3K activity.

Evidence accumulated over the past two decades has highlighted the presence of an autonomous nuclear inositol lipid metabolism and the fact that lipid molecules are important components of signaling pathways operating within the nucleus (1). PI3Ks, their lipid products, and AKT have been identified at the nuclear compartments of many cultured cells and some tissues (1, 32). Recent studies show that AKT is present in the nuclear compartment of human thyroid cancer cells (8, 10) and in primary lesions and metastases of TR$\beta^{PV/PV}$ mice (11). In the present study, we discovered that PI3K (p85α) was also localized in the nuclear compartments to activate the AKT–mTOR–p70^{S6K} pathway. Thus, the thyroid is another tissue in which PI3K could act in the cytoplasm as well as in the nucleus.

Although the regulation and signal transduction of PI3K in the cytoplasm are reasonably well defined (3), the control and actions of the nuclear PI3K remain unclear. Some of the important issues are how the nuclear PI3K is activated, what its interaction partners are, and what its final targets are. The present study identified a TRβ mutant, PV, as an interaction partner for the nuclear PI3K. PV is localized mainly in the nucleus and could therefore be recruited by the nuclear p85α to activate PI3K activity, leading to the activation of AKT–mTOR–p70^{S6K} signaling to contribute to translation and cell proliferation. One would envision that there are additional final targets of nuclear PI3K yet to be identified and their functions to be elucidated. The finding that the nuclear PI3K is activated by PV could be a valuable tool in further defining the role of nuclear PI3K *in vivo*.

In TR$\beta^{PV/PV}$ mice, the expression of PV causes resistance to thyroid hormone, pituitary tumors, and follicular carcinoma (33). Up to the present, studies aimed at understanding the molecular actions of TRβ mutants, including PV, have focused on their interference with the genomic actions of wild-type TRs. The fact that the interaction of PV with p85α results in the activation of PI3K, which was demonstrated in the present study, raises the possibility that, in addition to thyroid cancer, the nongenomic actions of PV could also contribute to the pathogenesis of resistance to thyroid hormone and pituitary tumors. The verification of this possibility will await future studies.

Materials and Methods

Mouse Strain. All aspects of animal care and experimentation were approved by the National Cancer Institute Animal Care and Use Committee. The mice harboring the TRβPV gene (TR$\beta^{PV/PV}$ mice) were prepared through homologous recombination, as described in ref. 15. TR$\beta^{PV/PV}$ mice used in the present study were offspring of many generations of intersibling mating over 6 years (>30 generations). Littermates were used in the phenotypic characterization in all studies. Genotyping was carried out by PCRs as described in ref. 15.

Western Blot Analysis. To separate nuclear or cytosolic fraction, pieces of thyroid tissue were homogenized five times in buffer A (350 mM sucrose/10 mM Hepes-KOH, pH 7.9/10 mM KCl/0.1 mM EDTA/0.5 mM DTT/0.15 mM spermine/0.5 mM spermidine) by using a Dounce homogenizer (loose) and then filtrated with gauze. The filtrated lysate was centrifuged for 10 min at 2,000 $\times$ *g*, and the supernatant was used as cytosolic fraction. The precipitation was washed twice with buffer A and homogenized in 1 ml of buffer A by using a Dounce homogenizer (tight). One milliliter of homogenized samples was laid on the 1 ml of buffer B (500 mM sucrose/10 mM Hepes-KOH, pH 7.9/10 mM KCl/0.1 mM EDTA/0.5 mM DTT/0.15 mM spermine/0.5 mM spermidine) and centrifuged for 15 min at 3,000 $\times$ *g* at 4°C. The precipitation was washed with buffer C (10 mM Hepes-KOH, pH 7.9/10 mM KCl/0.1 mM EDTA/0.5 mM DTT/0.15 mM spermine/0.5 mM spermidine) and resuspended with buffer D (550 mM KCl/20 mM Hepes-KOH, pH 7.9/1.1 mM $MgCl_2$/5 mM DTT/20% glycerol/260 mM sucrose). The lysate was incubated for 60

min with shaking and centrifuged for 60 min at 35,000 × *g* at 4°C. The supernatant was used for nuclear fraction. Determination of protein abundance of key regulators in PI3K–AKT pathways in the cytosolic and nuclear factions of thyroid extracts by Western blot analysis was carried out as described by Ying *et al.* (34). In coimmunoprecipitation experiments, the immunoprecipitation step and the subsequent Western blot analysis were carried out as described by Furumoto *et al.* (35).

Primary antibodies for phosphorylated S473 AKT (catalog no. 9271), total AKT (catalog no. 9272), phosphorylated S2448 mTOR (catalog no. 2971), total mTOR (catalog no. 2972), phosphorylated-Thr-421/S424 p70 S6 kinase (catalog no. 9204), and total p70 S6 kinase (catalog no. 9202) were purchased from Cell Signaling Technology. Anti-MMP2 (SC0729) antibodies were purchased from Santa Cruz Biotechnology. Anti-ILK (catalog no. 06-592) and anti-p85α (catalog no. 06-195) antibodies were purchased from Upstate Biotechnology. The total AKT and phospho-S473 AKT antibodies were used at a 1:1,000 dilution. The others were used at a 1:500 dilution. For control of protein loading, the blots were stripped and re-reacted with the antibodies against PDI (#3632), α-tubulin (T6199; Sigma), or PARP (SC7150; Santa Cruz Biotechnology).

PI3K Assay. Thyroid extracts prepared as described above were first immunoprecipitated with antibody against p85α, anti-TRβ1, or PV. PI3K activity in the immunocomplexes was determined by using a PI3K ELISA kit according to the manufacturer's instructions (Echelon Biosciences).

Primary Thyroid Cultured Cells. Primary thyroid cells from wild-type and TR$\beta^{PV/PV}$ mice were prepared in a manner similar to that described by Zimonjic *et al.* (36), but with a slight modification in the cultured media. Cells were cultured in Coon's modified Ham's F-12 medium supplemented with 5% calf serum and mixed with six hormones containing 10 μg/ml insulin, 0.4 ng/ml cortisol, 5 μg/ml transferrin, 10 ng/ml glycyl-L-histidyl-L-lysine acetate, 10 ng/ml somatostatin, and 1 milliunit/ml thyroid-stimulating hormone (Sigma).

GST-Binding Assay. Binding of ^{35}S-labeled TRβ1 or PV to GST–p85α was carried out as described in ref. 37, with modifications. The plasmid of pGST–p85α was a gift from James Liao (Brigham and Women's Hospital, Harvard Medical School, Boston). *In vitro* translated ^{35}S-labeled TRβ1 and PV were synthesized by using a TNT kit (Promega) and incubated with GST–p85α at 4°C for 24 h with constant shaking. The beads were washed five times, and the bound proteins were analyzed by SDS/PAGE.

Fluorescence Confocal Microscopy. Subcellular localization of TRβ1, PV, and p85α in primary thyroid tumor cells was evaluated by using fluorescence confocal microscopy. One day after plating, 6×10^4 cells per well in chamber slides (catalog no. 154461; Nalge Nunc International), cells were washed twice in PBS, fixed with freshly prepared 4% paraformaldehyde (10 min at room temperature), and permeabilized with 0.2% Triton X-100 in PBS (10 min at room temperature). Nonspecific binding of the antibodies was blocked with 3% BSA before incubation with the monoclonal anti-TRβ1 and PV antibodies (J52) and the anti-p85α antibodies (SC423; Santa Cruz Biotechnology) at 4°C overnight. The cells were subsequently incubated with 1.0 μg/ml Alexa Fluor 488 fragment of goat anti-mouse IgG (A11017; Molecular Probes) or tetra methyl rhodamine goat anti-rabbit IgG (T2769; Molecular Probes). Nuclei were also stained with DAPI (Vector Laboratories). Laser confocal scanning images were captured by using an Ultraview (PerkinElmer) confocal head on a Zeiss TV200 inverted microscope.

We thank Dr. James Liao for the pGST–p85α plasmid. This research was supported in part by the Intramural Research Program of the Center for Cancer Research of the National Cancer Institute, National Institutes of Health.

1. Neri, L. M., Borgatti, P., Capitani, S. & Martelli, A. M. (2002) *Biochim. Biophys. Acta* **1584,** 73–80.
2. Shepherd, P. R., Withers, D. J. & Siddle, K. (1998) *Biochem. J.* **333,** 471–490.
3. Wymann, M. P. & Marone, R. (2005) *Curr. Opin. Cell Biol.* **17,** 141–149.
4. Sansal, I. & Sellers, W. R. (2004) *J. Clin. Oncol.* **22,** 2954–2963.
5. Eng, C. (2003) *Hum. Mutat.* **22,** 183–198.
6. Dahia, P. L., Marsh, D. J., Zheng, Z., Zedenius, J., Komminoth, P., Frisk, T., Wallin, G., Parsons, R., Longy, M., Larsson, C., *et al.* (1997) *Cancer Res.* **57,** 4710–4713.
7. Liaw, D., Marsh, D. J., Li, J., Dahia, P. L., Wang, S. I., Zheng, Z., Bose, S., Call, K. M., Tsou, H. C., Peacocke, M., *et al.* (1997) *Nat. Genet.* **16,** 64–67.
8. Ringel, M. D., Hayre, N., Saito, J., Saunier, B., Schuppert, F., Burch, H., Bernet, V., Burman, K. D., Kohn, L. D. & Saji, M. (2001) *Cancer Res.* **61,** 6105–6111.
9. Miyakawa, M., Tsushima, T., Murakami, H., Wakai, K., Isozaki, O. & Takano, K. (2003) *Endocr. J.* **50,** 77–83.
10. Vasko, V., Saji, M., Hardy, E., Kruhlak, M., Larin, A., Savchenko, V., Miyakawa, M., Isozaki, O., Murakami, H., Tsushima, T., *et al.* (2004) *J. Med. Genet.* **41,** 161–170.
11. Kim, C. S., Vasko, V. V., Kato, Y., Kruhlak, M., Saji, M., Cheng, S. Y. & Ringel, M. D. (2005) *Endocrinology* **146,** 4456–4463.
12. Suzuki, H., Willingham, M. C. & Cheng, S. Y. (2002) *Thyroid* **12,** 963–969.
13. Ying, H., Suzuki, H., Zhao, L., Willingham, M. C., Meltzer, P. & Cheng, S. Y. (2003) *Cancer Res.* **63,** 5274–5280.
14. Ying, H., Suzuki, H., Furumoto, H., Walker, R., Meltzer, P., Willingham, M. C. & Cheng, S. Y. (2003) *Carcinogenesis* **24,** 1467–1479.
15. Kaneshige, M., Kaneshige, K., Zhu, X., Dace, A., Garrett, L., Carter, T. A., Kazlauskaite, R., Pankratz, D. G., Wynshaw-Boris, A., Refetoff, S., *et al.* (2000) *Proc. Natl. Acad. Sci. USA* **97,** 13209–13214.
16. Parrilla, R., Mixson, A. J., McPherson, J. A., McClaskey, J. H. & Weintraub, B. D. (1991) *J. Clin. Invest.* **88,** 2123–2130.
17. Yen, P. M. (2003) *Trends Endocrinol. Metab.* **14,** 327–333.
18. Meier, C. A., Parkison, C., Chen, A., Ashizawa, K., Meier-Heusler, S. C., Muchmore, P., Cheng, S. Y. & Weintraub, B. D. (1993) *J. Clin. Invest.* **92,** 1986–1993.
19. Simoncini, T., Hafezi-Moghadam, A., Brazil, D. P., Ley, K., Chin, W. W. & Liao, J. K. (2000) *Nature* **407,** 538–541.
20. Cao, X., Kambe, F., Moeller, L. C., Refetoff, S. & Seo, H. (2005) *Mol. Endocrinol.* **19,** 102–112.
21. Lin, K.-H., Parkison, C., McPhie, P. & Cheng, S.-Y. (1991) *Mol. Endocrinol.* **5,** 485–492.
22. Zhang, X. Y., Kaneshige, M., Kamiya, Y., Kaneshige, K., McPhie, P. & Cheng, S. Y. (2002) *Mol. Endocrinol.* **16,** 2077–2092.
23. Wetzker, R. & Rommel, C. (2004) *Curr. Pharm. Des.* **10,** 1915–1922.
24. Asnaghi, L., Bruno, P. Priulla, M. & Nicolin, A. (2004) *Pharmacol. Res.* **50,** 545–549.
25. Persad, S. & Dedhar, S. (2003) *Cancer Metastasis Rev.* **22,** 375–384.
26. Edwards, L. A., Shabbits, J. A., Bally, M. & Dedhar, S. (2004) *Cancer Treat. Res.* **119,** 59–75.
27. Grashoff, C., Thievessen, I., Lorenz, K., Ussar, S. & Fassler, R. (2004) *Curr. Opin. Cell Biol.* **16,** 565–571.
28. Brinckerhoff, C. E. & Matrisian, L. M. (2004) *Nat. Rev. Mol. Cell Biol.* **3,** 207–214.
29. Turpeenniemi-Hujanen, T. (2005) *Biochimie* **87,** 287–297.
30. Beeton, C. A., Das, P., Waterfield, M. D. & Shepherd, P. R. (1999) *Mol. Cell Biol. Res. Commun.* **1,** 153–157.
31. Kang, Q., Cao, Y. & Zolkiewska, A. (2001) *J. Biol. Chem.* **276,** 24466–24472.
32. Irvine, R. F. (2003) *Nat. Rev. Mol. Cell Biol.* **4,** 349–360.
33. Cheng, S. Y. (2005) *Trends Endocrinol. Metab.* **16,** 176–182.
34. Ying, H., Furuya, F., Willingham, M. C., Xu, J., O'Malley, B. W. & Cheng, S. Y. (2005) *Mol. Cell. Biol.* **25,** 7687–7695.
35. Furumoto, H., Ying, H., Chandramouli, G. V., Zhao, L., Walker, R. L., Meltzer, P. S., Willingham, M. C. & Cheng, S. Y. (2005) *Mol. Cell. Biol.* **25,** 124–135.
36. Zimonjic, D. B., Kato, Y., Ying, H., Popescu, N. C. & Cheng, S. Y. (2005) *Cancer Genet. Cytogenet.* **161,** 104–109.
37. Yap, N., Yu, C. L. & Cheng, S. Y. (1996) *Proc. Natl. Acad. Sci. USA* **93,** 4273–4277.